Biochimica et Biophysica Acta 1840 (2014) 951–957

Contents lists available at ScienceDirect

Biochimica et Biophysica Acta

journal homepage: www.elsevier.com/locate/bbagen

Genetically encoded fluorescent indicator for imaging NAD$^+$/NADH ratio changes in different cellular compartments

Dmitry S. Bilan [a,b], Mikhail E. Matlashov [a,b], Andrey Yu. Gorokhovatsky [b], Carsten Schultz [c], Grigori Enikolopov [a,d], Vsevolod V. Belousov [a,b,*]

[a] Moscow Institute of Physics and Technology, 141700 Moscow Region, Russia
[b] Shemyakin-Ovchinnikov Institute of Bioorganic Chemistry, 117997 Moscow, Russia
[c] European Molecular Biology Laboratory, 69117 Heidelberg, Germany
[d] Cold Spring Harbor Laboratory, 11724 Cold Spring Harbor, NY, USA

ARTICLE INFO

Article history:
Received 23 May 2013
Received in revised form 19 November 2013
Accepted 20 November 2013
Available online 25 November 2013

Keywords:
NAD$^+$/NADH ratio
Fluorescent probe
Redox sensor

ABSTRACT

Background: The ratio of NAD$^+$/NADH is a key indicator that reflects the overall redox state of the cells. Until recently, there were no methods for real time NAD$^+$/NADH monitoring in living cells. Genetically encoded fluorescent probes for NAD$^+$/NADH are fundamentally new approach for studying the NAD$^+$/NADH dynamics.
Methods: We developed a genetically encoded probe for the nicotinamide adenine dinucleotide, NAD(H), redox state changes by inserting circularly permuted YFP into redox sensor T-REX from *Thermus aquaticus*. We characterized the sensor in vitro using spectrofluorometry and in cultured mammalian cells using confocal fluorescent microscopy.
Results: The sensor, named RexYFP, reports changes in the NAD$^+$/NADH ratio in different compartments of living cells. Using RexYFP, we were able to track changes in NAD$^+$/NADH in cytoplasm and mitochondrial matrix of cells under a variety of conditions. The affinity of the probe enables comparison of NAD$^+$/NADH in compartments with low (cytoplasm) and high (mitochondria) NADH concentration. We developed a method of eliminating pH-driven artifacts by normalizing the signal to the signal of the pH sensor with the same chromophore.
Conclusion: RexYFP is suitable for detecting the NAD(H) redox state in different cellular compartments.
General significance: RexYFP has several advantages over existing NAD$^+$/NADH sensors such as smallest size and optimal affinity for different compartments. Our results show that normalizing the signal of the sensor to the pH changes is a good strategy for overcoming pH-induced artifacts in imaging.

1. Introduction

Aerobic organisms produce energy by oxidizing fuel molecules. The oxidized form of nicotinamide adenine dinucleotide (NAD$^+$) becomes converted to NADH by accepting reducing equivalents in the form of electrons and hydrogen atoms from oxidized compounds in dehydrogenase reactions. Reoxidation of NADH takes place mainly in electron transport chains (ETCs) that use electrons to reduce molecular oxygen and to produce energy in the form of ATP. The most important metabolic parameter is the exact ratio of the oxidized to the reduced forms of the cofactor. In mitochondria, NAD$^+$/NADH ratios vary from 1 to 7–8, while the cytosolic NAD$^+$/NADH index varies over a wider range, from 1 to up to 700 [1–3].

The ratio of NAD$^+$/NADH is a key indicator that reflects the overall redox state of the cells. For many decades, it has been thought that the major role of NAD(H) is controlling cellular energy and metabolism. Later, it turned out that NAD$^+$ and NADH exert their biological effects by regulating a wide range of NAD$^+$/NADH-dependent enzymes, including dehydrogenases, mono(ADP-ribosyl)transferases, poly(ADP-ribose) polymerases (PARPs), ADP-ribosyl cyclases, and sirtuins [3]. Processes regulated by NAD$^+$ and NADH include, but are not limited to, aging [3], cell death [4,5], Ca^{2+} signaling [6,7] and gene expression [8].

Until recently, UV and two-photon microscopy were the only methods for NAD(P)H imaging in living cells in real time [9–13]. However, these methods do not discriminate NADH from oxidized flavins [10], are relatively photodamaging for the cells [14–17], and fail to report NAD$^+$/NADH pair redox state. Recently, genetically encoded fluorescent probes for NAD$^+$/NADH have been developed by integrating fluorescent proteins into Rex family domains [18,19]. Bacterial species utilize the family of Rex transcriptional repressors to sense oxygen availability via NAD(H) redox state [20]. Rex is very sensitive to changes in free NADH within cells. In the presence of oxygen, when the index of NAD$^+$/NADH is high, Rex forms a stable complex with DNA and one molecule of NAD$^+$, acting as a repressor of its target genes (cydABC, nuoA-D, rex-hemACD) [21]. However, with a fall in oxygen concentration the pool of the NAD(H) becomes more reduced and NADH displaces NAD$^+$ in Rex due to much higher affinity of Rex for NADH compared to NAD$^+$. NADH binding leads to conformational changes in

* Corresponding author at: Moscow Institute of Physics and Technology, 141700 Moscow Region, Russia.
E-mail address: vsevolod.belousov@gmail.com (V.V. Belousov).

0304-4165/$ – see front matter © 2013 Elsevier B.V. All rights reserved.
http://dx.doi.org/10.1016/j.bbagen.2013.11.018

the structure of the protein and its subsequent dissociation from the complex with DNA [20,21].

Existing genetically encoded NAD^+/NADH sensors are based on insertion of circularly permuted fluorescent proteins (cpFP) between the Rex monomers constituting the functional Rex dimer, making the expression construct rather large [18,19]. One of them, Peredox [18], incorporates an additional RFP molecule to obtain ratiometric readout — making the expression construct even bigger.

When tested in the mitochondria, Peredox failed to report changes in NAD^+/NADH ratio due to its extremely high sensitivity to NADH [18]. Frex versions for mitochondria and cytoplasm differ from each other, complicating direct comparison of the NAD^+/NADH changes in these compartments [19].

We developed a genetically encoded fluorescent sensor for detection of the NAD^+/NADH ratio in cells using the alternative approach of inserting cpYFP into the loop of a monomer of the Rex homolog from *Thermus aquaticus* (T-Rex), between its nucleotide-binding Rossmann fold and DNA-binding WH domain. This scheme was used in our laboratory to make a probe for H_2O_2 (HyPer) [22] and later by others in making probes for ATP/ADP ratio [23], organic hydroperoxide [24], and carbon monoxide [25]. The resulting sensor, named RexYFP, reported real-time changes in NAD^+/NADH ratio both in vitro and in different compartments of mammalian cells, including mitochondrial matrix. The molecular weight of the RexYFP monomer is 1.5- to 2-fold lower than that of Frex and Peredox. Since the signal of cpYFP-based sensors depends on pH, we utilized HyPer C199S [22], also known as SypHer [26], to control pH changes in parallel experiments. Normalizing the signal of RexYFP to the signal of SypHer eliminates pH-related artifacts.

2. Materials and methods

2.1. Generation of RexYFP construction

T-Rex was amplified from genomic DNA of *Thermus thermophilus*. We integrated cpYFP between different positions in the sequence of T-Rex to obtain several versions of T-Rex–cpYFP constructions. To do this, we amplified corresponding fragments of T-Rex and full-sized cpYFP. Fragments were combined into a whole construct by "overlap extension" PCR. We performed ligation of all T-Rex–cpYFP constructs into the vector pQe30 (Qiagen) or pC1 (Clontech) with or without mitochondrial localization sequence. To improve properties of some of the versions, we carried out random mutagenesis using a kit designed for this purpose (Clontech). The selection of fluorescent clones expressing the sensor was carried out using a fluorescence binocular microscope (Olympus US SZX12). In the next stage, we evaluated spectral characteristics of selected clones using a fluorescence spectrophotometer (Varian Cary Eclipse). For this, we detected excitation spectra of each test version in the range of 400–510 nm (emission 530 nm). Then we extracted proteins to determine the sensitivity of selected versions to NADH and NAD^+.

2.2. Characterization of RexYFP in vitro

We purified selected versions of T-Rex–cpYFP using standard metal affinity technique. *Escherichia coli* XL1Blue cells expressing recombinant plasmids pQE30-T-Rex–cpYFP on agar plates and incubated overnight at 37 °C. Next day the cells were subcultured in 200 mL of LB medium and grown overnight at room temperature. The cells were collected by 15 min centrifugation at 2000 *g* and resuspended in 40 mM Tris–HCl buffer, pH 7.4. The cells were sonicated using Sonic Dismembrator (Fisher Scientific) and lysates were centrifugated for 30 min at 18000 *g* at 4 °C. Soluble proteins containing N-terminal His-tag were purified using metal-affinity resin TALON (Clontech). For this, we applied the samples to the column with TALON and eluted target protein with buffer containing 300 mM imidazole. To remove imidazole we performed gel filtration chromatography using Micro Bio-Spin P-30 Tris Chromatography Columns (Bio Rad). An aliquot of the purified protein was diluted in a buffer of 40 mM Tris–HCl, 150 mM NaCl, pH 7.5. We detected the absorption spectra using a spectrophotometer (Varian Cary 100 Bio) from 300 to 520 nm and the excitation spectra using a fluorescence spectrophotometer (Varian Cary Eclipse) from 350 to 510 nm and emission 530 nm. We added an excess of NAD^+ (Sigma) (250 nM protein and 100 μM NAD^+) to the sample. Then in the same sample we gradually increased the concentration of NADH (Sigma) to 25, 50, 100, 250 and 500 nM. We chose the most NADH-sensitive version, called RexYFP. Similarly, we tested the affinity of RexYFP to ATP (AppliChem) and NADPH (Sigma). We used a coupled enzyme system to determine the dependence of RexYFP signal on the NAD^+/NADH ratio in the sample (see above).

2.3. Cell culture and transfection

HeLa and HEK293 cells (ATCC) were cultured in DMEM, High Glucose (Gibco) with 10% FCS (Gibco) at 37 °C in a 5% CO_2 atmosphere. For imaging experiments, cells were seeded into μ-Slide 8 well (ibidi). After 24 h, cells were transfected using FuGene6 transfection reagent (Promega); then, 6–7 h after transfection, cell medium was replaced by fresh medium. For experiments with Peredox probe, cells were transfected with pcDNA3.1-Peredox-mCherry plasmid (Addgene 32383).

2.4. Fluorescence microscopy

We used a confocal fluorescence microscope (Perkin Elmer UltraView Vox Spinning Disk) to visualize the fluorescence of transfected cells 24–48 h after transfection with 40× (1.30 NA) and 60× (1.42 NA) objectives (for visualization of mitochondrial RexYFP). Microscopy of cells was carried out at 37 °C in Live Cell Imaging Solution (Gibco) with addition of glucose (Sigma) (final concentration 2 g/L). Fluorescence detection was carried out using 488 laser line (also 405 and 560 for Peredox). For RexYFP we used 488 laser with about 20% intensity and 150 ms of exposure; RexYFP with mitochondrial localization has weaker fluorescence, so we used 488 laser with about 30% intensity and 300 ms of exposure. The final processing of images was performed using the program ImageJ.

3. Results

3.1. Construction and spectral properties of RexYFP

We chose T-Rex protein from *T. aquaticus* [20] as the NAD^+/NADH ratio sensing domain to make the fluorescent indicator. T-Rex exists in two conformations depending on the level of NADH in the system. We integrated cpYFP into the T-Rex moiety believing that changes in T-Rex conformation will cause changes in the spectrum of the fluorescent protein in the T-Rex–cpYFP chimera — enabling monitoring of NAD^+/NADH dynamics. We have created several chimeric proteins in which the fluorescent protein was inserted into different positions of T-Rex. Upon expression in *E. coli* cells, most clones containing chimeric proteins displayed weak or undetectable fluorescence. However, clones that expressed proteins in which cpYFP was integrated between residues 79–80, 99–100 and 166–167 of T-Rex were fluorescent. The T-Rex–79–80–cpYFP protein demonstrated the highest dynamic range of fluorescence intensity upon intensive aeration of the media containing expressing *E. coli* cells. We subjected T-Rex–79–80–cpYFP to random mutagenesis to facilitate brightness and maturation at physiological temperatures. The version with L169P, Y175N, and D313G mutations was named RexYFP and chosen for the subsequent experiments (Fig. 1A). All mutations in the structure of RexYFP were located in the cpYFP part of the sensor.

The fluorescence spectrum of RexYFP has a single excitation peak at 490 nm and an emission peak with a maximum at 516 nm (Fig. 1B).

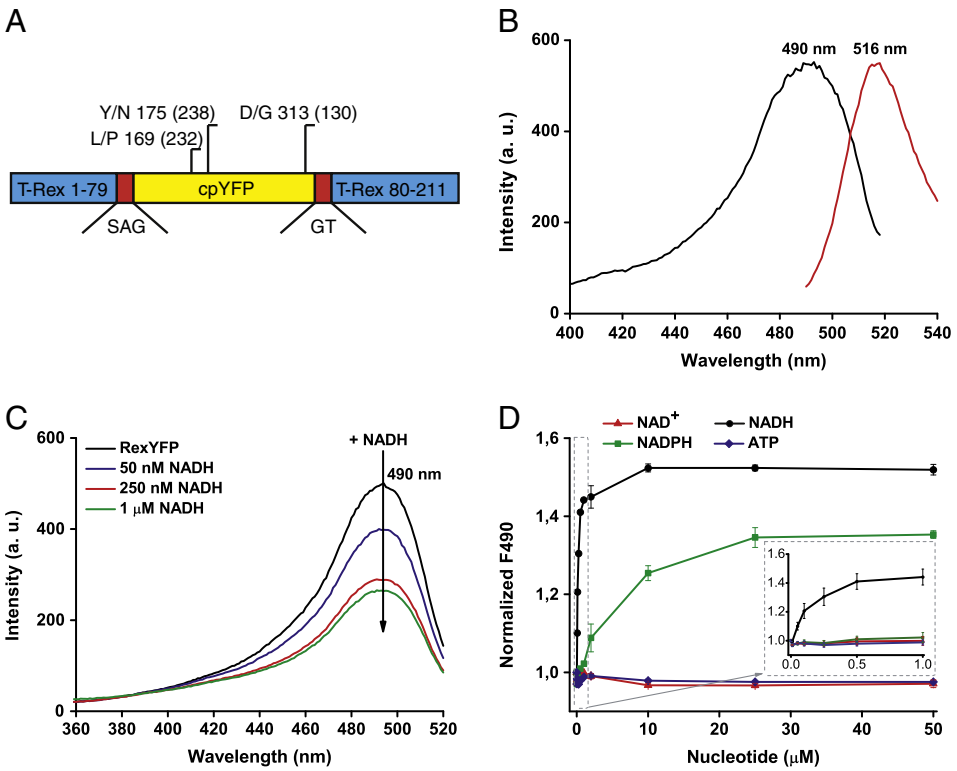

Fig. 1. A) Diagram of the RexYFP structure. RexYFP consists of cpYFP (yellow) integrated between residues 79 and 80 of T-Rex (blue) via short polypeptide linkers SAG and GT (red). The diagram shows mutations in the structure of RexYFP (numbers in parentheses indicate the position for EYFP). B) Fluorescence spectra of RexYFP. Excitation spectrum has a maximum at 490 nm. Emission spectrum has a maximum at 516 nm. C) Excitation spectrum of RexYFP (250 nM) in Tris–HCl (pH 7.5) with 150 mM NaCl and 10 mM $MgCl_2$ upon addition of NADH (50, 250, 1000 nM) to the probe. Emission was measured at 530 nm. D) Dependence of RexYFP signal on concentrations of various nucleotides (NAD^+, NADH, NADPH, ATP) in range of concentration from 10 nM to 50 μM in the probe (Tris–HCl (pH 7.5), 150 mM NaCl, 10 mM $MgCl_2$). The RexYFP signal is expressed as 1/F490. Plotted line for each type of nucleotide is the result of five independent experiments.

3.2. Determination of RexYFP sensitivity to NAD^+/NADH changes

Since T-Rex has high affinity for NADH and co-purifies with bound NADH [27], the ligand was removed from purified RexYFP by ammonium sulfate precipitation under acidic conditions before the experiment. Adding a small amount of NADH (50 nM) to the sample with apo-RexYFP (250 nM) decreased the fluorescence intensity of the probe excited in the 490 nm range. Fluorescence intensity progressively decreased with increasing concentration of NADH (Fig. 1C). We further defined RexYFP signal as 1/F490. Therefore, an increase of NADH in the system leads to an increase in RexYFP signal.

Rossmann-fold-based nucleotide-binding domains differ in their sensitivity to various nucleotides. We tested the measured affinity of the RexYFP to different nucleotides, namely NADH, NAD^+, NADPH and ATP, each ranging from 10 nM to 50 μM (Fig. 1D). We found that even large concentrations of NAD^+ and ATP did not substantially change RexYFP fluorescence. NADH binding caused changes of the signal with an affinity constant (K′) of 180 nM. NADPH also shifted F490, but with much lower affinity (K'_{NADPH} = 6.2 μM). However, since the $NADP^+$/NADPH pool is more reduced compared to the NAD^+/NADH in the cytoplasm [1], potential interference from NADPH in the living cell cannot be excluded.

Natural T-Rex is able to bind NAD^+ and NADH with different affinities [20]. Under physiological conditions in the cytoplasm of mammalian cells, the approximate value of the ratio between free NAD^+ to NADH ranges from 1 to 700 [1–3]. Since NAD^+ is always present in cells in relatively high concentrations compared to NADH, the NAD^+- bound state can be assumed as a physiological "ground" state of the probe. We used a coupled enzymatic system to determine the RexYFP sensitivity to NAD^+/NADH changes (Fig. 2A). In this system glucose becomes converted to glucose-6-phosphate in the reaction catalyzed by hexokinase. Glucose-6-phosphate gets converted to 6-phosphogluconate by yeast glucose-6-phosphate dehydrogenase that uses the reducing equivalent to reduce NAD^+ [28].

In each series of experiments we used different concentrations of RexYFP (100, 250, 750 nM) in the reaction mixture containing glucose, Mg-ATP, NAD^+ and glucose-6-phosphate dehydrogenase, and started the reaction by adding hexokinase. The formation of NADH caused an increase in absorption at 340 nm simultaneous with a decrease in the 490 nm excitation peak of RexYFP in the same sample (Fig. 2B, C). We found that RexYFP responds to even small amounts of NADH appearing at the initial stages of the reaction. Thus, being a part of the probe, the T-Rex domain retained its ability to respond to small changes in NADH concentration against the excess of NAD^+ and ATP.

The RexYFP signal was not dependent on the sensor concentration in the sample. In all the in vitro tests we buffered pH in the reaction mixture in order to exclude pH effects on the signal of the sensor.

3.3. RexYFP in eukaryotic cells: solving the problem of pH dependence

To test performance of the probe in eukaryotic cells, we expressed RexYFP in HeLa and HEK293 cell lines.

Fluorescence of RexYFP depends on pH, as in other sensors based on cpYFP. Many intracellular processes may cause fluctuations of cellular pH. Decrease in pH leads to a decrease in fluorescence of RexYFP excited at 490 nm, thus mimicking rise in NADH. To account for the effect of pH on the signal of RexYFP, we used the control protein HyPer-C199S (SypHer) [22,26]. HyPer is a genetically encoded sensor for detecting H_2O_2. Mutation C199S makes the sensor insensitive to H_2O_2. However, the sensor retains intrinsic pH sensitivity. We determined the pH dependence of the fluorescence intensity of RexYFP and HyPer-C199S at 490 nm. The sensors differ in pKa ($pKa_{HyPer\text{-}C199S}$ = 8.5;

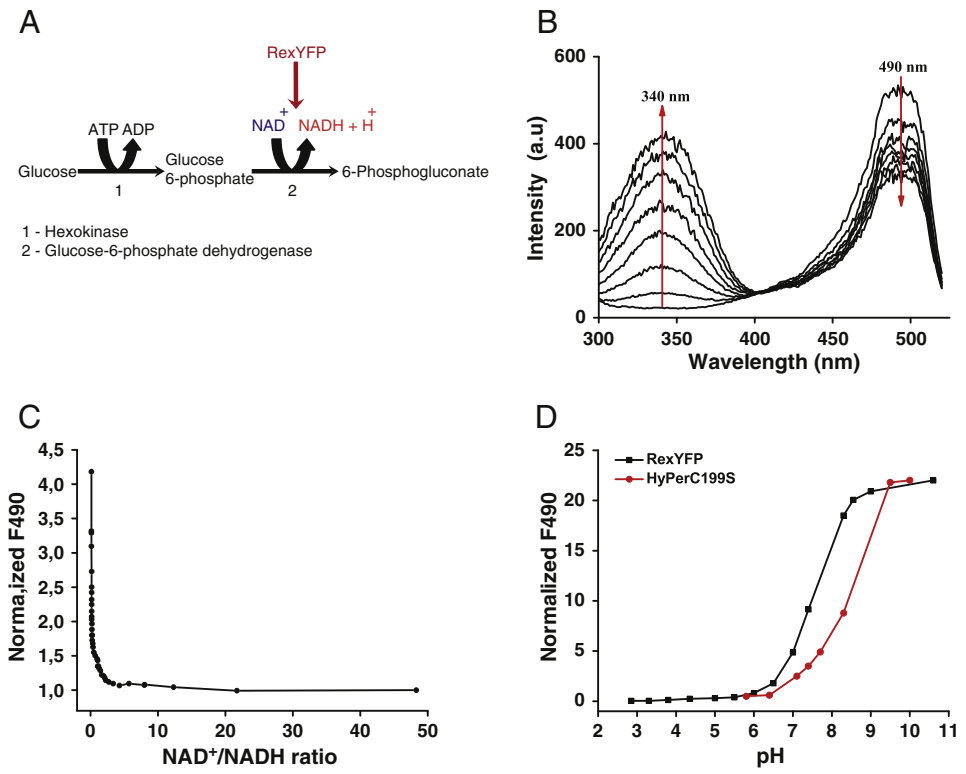

Fig. 2. A) The scheme of a coupled enzymatic system used to determine the dependence of the RexYFP signal on the NAD^+/NADH ratio. B) Dynamics of changes in the excitation spectrum of the sample containing RexYFP and components of running coupled system. C) Dependence of the RexYFP signal from the NAD^+/NADH ratio. Values of the RexYFP signal and the NAD^+/NADH ratio were calculated from the excitation spectra, which were detected in the sample containing RexYFP and components of the coupled system every 30 s, (3 experiments). D) The pH dependence of the fluorescence intensity (F490) of cpYFP chromophore in HyPer-C199S (red line) and RexYFP (black line), (2 experiments).

$pKa_{RexYFP} = 7.6$), but the amplitudes of the fluorescence changes are very similar (~8 fold) between the probes in the physiological pH range between 6.5 and 8.0 (Fig. 2D). Therefore, RexYFP signal normalized to HyPer-C199S signal provides maximally reliable information about the NAD^+/NADH ratio changes in the cells.

In addition, pH could influence nucleotide binding properties of T-Rex [18]. Conserved residue Y98 of T-Rex, which is located near the nicotinamide moiety of NADH [27], may participate in proton transfer [29]. To minimize the effect of pH on NADH binding of RexYFP, we used a strategy previously applied to Peredox reporter: substituting Tyr 98 to Trp [18].

In order to validate our approach to pH influence compensation, we added pyruvate and lactate to the cells expressing RexYFP and, at the same time, to the cells expressing HyPer-C199S. Using μ-Slide 8 well we were able to detect the signals from the cells transfected with different sensors simultaneously by using the multi-position time-lapse mode of the confocal fluorescence microscope. Transport of both lactate and pyruvate via plasma membrane caused acidification of the cytoplasm of the cells consistent with a proton symport with these substrates [30,31]. We normalized the RexYFP F490 to the HyPer-C199S F490. Both signals were averaged over a large number of cells. Normalized RexYFP signal ($F490_{RexYFP}/F490_{HyPer\text{-}C199S}$) is independent of pH fluctuations. We compared head-to-head pH-normalized RexYFP signals with those of the previously published sensor Peredox [18] responding to the addition of pyruvate and lactate (Fig. 3A, B). Peredox is a chimeric protein in which cpFP T-Sapphire inserted between the monomers of the T-Rex dimer. Upon rise of NADH fluorescence of T-Sapphire in Peredox increases. To enable ratiometric readout Peredox is tandemly fused to mCherry. Therefore Peredox signal is calculated as F405 / F561 [18].

After the addition of 5 mM pyruvate, both RexYFP and Peredox detected a decrease in cytoplasmic NADH. Excess lactate (20 mM) in the medium led to a rapid increase in NADH. But in the next 15 min the balance between NAD^+ and NADH returned to the initial level. Similar shapes and amplitudes of responses from both sensors argue for utility of pH-normalized RexYFP signals in monitoring of NAD^+/NADH ratio.

3.4. Spread of NAD^+/NADH ratio changes from mitochondria to cytoplasm

Mitochondria are the major NADH consumers in the cell. However, whether the changes in the redox state of the mitochondrial matrix spread to the cytoplasm is not clear. We used rotenone to inhibit complex I of the mitochondrial respiratory chain and detected changes in NAD^+/NADH ratio in the cytoplasm of HeLa cells using RexYFP and Peredox. Both indicators detected a rotenone-induced increase in cytosolic NADH, indicating that reduction of the NAD(H) fraction in the matrix does spread to the cytoplasm (Fig. 3C). The Peredox signal reached its maximal response earlier than RexYFP. This could be explained by the higher affinity for NADH of Peredox [18] compared to RexYFP. Inhibition of the respiratory chain leads to slower NAD(H) pool reduction compared to lactate addition.

3.5. Mitochondrial matrix vs. cytoplasm changes in nicotinamide adenine dinucleotide redox state

The NAD^+/NADH ratio is about 100-fold lower in the mitochondria than in the cytoplasm [1]. Peredox cannot be used to detect the dynamic of NAD^+/NADH ratio in mitochondria due to its high affinity for NADH [18]. RexYFP has lower affinity, so we decided to test its performance in the mitochondria. We fused RexYFP to N-terminal mitochondrial localization sequence (mitoRexYFP). We simultaneously imaged HyPer-C199S with mitochondrial localization (mitoSypHer) to normalize the mitoRexYFP signal to pH changes.

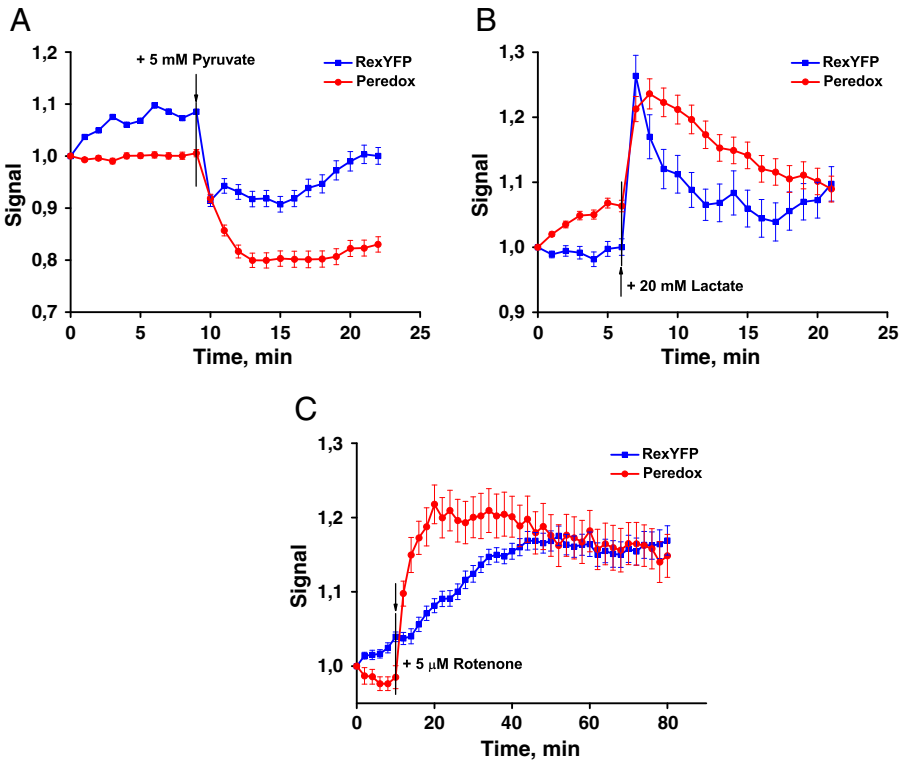

Fig. 3. Responses of RexYFP (blue line) and Peredox (red line) to the addition of A) 5 mM pyruvate B) 20 mM lactate. HEK293 cells transiently expressing the sensors were imaging in presence of glucose (2 g/L). Peredox signal is calculated as F405/F561; RexYFP as $F490_{HyPer\text{-}C199S}/F490_{RexYFP}$. Signal values of RexYFP and Peredox were normalized to the initial value. Signals were averaged from 55 cells for RexYFP and 38 cells for Peredox in 3 experiments with pyruvate; from 36 cells for RexYFP and 50 cells for Peredox in 3 experiments with lactate. Error bars indicate standard error of mean. C) RexYFP (blue line) and Peredox (red line) responses in the cytoplasm of HeLa cells incubated with 5 μM rotenone. Signals were averaged from 43 cells for RexYFP and 57 cells for Peredox in 3 experiments; error bars indicate standard error of mean.

We explored effects of the mitochondrial respiratory chain inhibitors on the dynamics of NAD^+/NADH ratio in the mitochondria and cytoplasm of the cells.

We compared effects of a rotenone-induced (25 μM) inhibition of the mitochondrial respiratory chain on NAD(H) redox state in both compartments. We found that complex I inhibition leads to the widespread increase of NADH, with somewhat higher increase in the mitochondrial matrix (Fig. 4A).

Addition of the complex II inhibitor 3-nitropropionic acid (1 mM) to the cells decreased NADH concentrations in mitochondria. At the same time, NAD^+/NADH ratio in the cytoplasm remained stable (Fig. 4B).

The mitochondrial uncoupler carbonyl cyanide m-chlorophenylhydrazone (CCCP) in concentration of 5 μM led to oxidation of NADH in the mitochondria while in the cytoplasm NADH slightly increased (Fig. 4C). CCCP caused acidification in both the mitochondrial matrix and the cytoplasm. Subsequent addition of 25 μM rotenone to the same cells increased NADH in both compartments (Fig. 4D). Notably, the effect of the rotenone was more rapid in the cytoplasm than in mitochondria.

Taken together, our findings show that RexYFP fluorescence ratio normalized to pH changes provides a suitable readout for the detection of NAD^+/NADH dynamics in different cellular compartments.

4. Discussion

The redox state of nicotinamide adenine dinucleotide, NAD(H), is a key parameter on a crossroad of metabolic and signaling pathways. We developed the genetically encoded fluorescent sensor RexYFP to measure NAD^+/NADH ratios within cells. RexYFP is made using a single subunit of transcription factor T-Rex from *T. aquaticus* [20]. We inserted cpYFP into the loop between nucleotide- and DNA-binding domains. Thus, RexYFP is much smaller in size per monomer compared to the previously published sensors Peredox (based on two subunits of T-Rex and two fluorescent proteins) [18] and Frex (based on two subunits of B-Rex and fluorescent protein) [19]. The small size of the sensor molecule may be important for targeting subcellular structures and for its performance in chimeric proteins. As the proteins are transported into the mitochondrial matrix as monomers, smaller size of the monomer could improve targeting. The same is probably true for targeting to other compartments. Rex domains are dimers [20,21] and the same is expected for RexYFP. Therefore, the protein unit (dimer) of RexYFP is larger in size than Frex and similar to ratiometric Peredox-mCherry. Potential benefit of two FPs per dimer of RexYFP is twice higher brightness per sensor unit. However dimerization of the probe can affect proper function of target proteins in fusions. We recommend to use RexYFP in chimeric proteins with careful attention.

We tested RexYFP in vitro and determined its specificity for NADH. RexYFP has an affinity constant (K′) for NADH of 180 nM. For comparison, Peredox has an affinity for NADH less than 5 nM, which makes this sensor unusable in the mitochondrial matrix (18). Frex has several variations with different affinities: Frex (3.7 μM), FrexH (40 nM), and version C3L194K (50 μM); each suited to different experiments [19]. RexYFP, with its affinity constant of 180 nM, has an intermediate position in a line of affinities between Peredox and Frexes: 5 nM (Peredox) < 40 nM (FrexH) < 180 nM (RexYFP) < 3.7 μM (Frex) < 50 μM (C3L194K). Whereas Peredox can be used only in the cytoplasm [18] and different versions of Frex were used to monitor NADH changes in the cytoplasm and in the mitochondria [19], RexYFP is suitable for NAD^+/NADH detection in both of these compartments.

We determined that only NADH and NADPH binding cause changes in RexYFP signals. Affinity constants for NADH and NADPH are 180 nM and 6.2 μM, respectively. The difference in the affinity constants argues for an almost exclusive role of NADH in changing the sensor signal. However, $NADP^+$/NADPH pool is more reduced compared to the

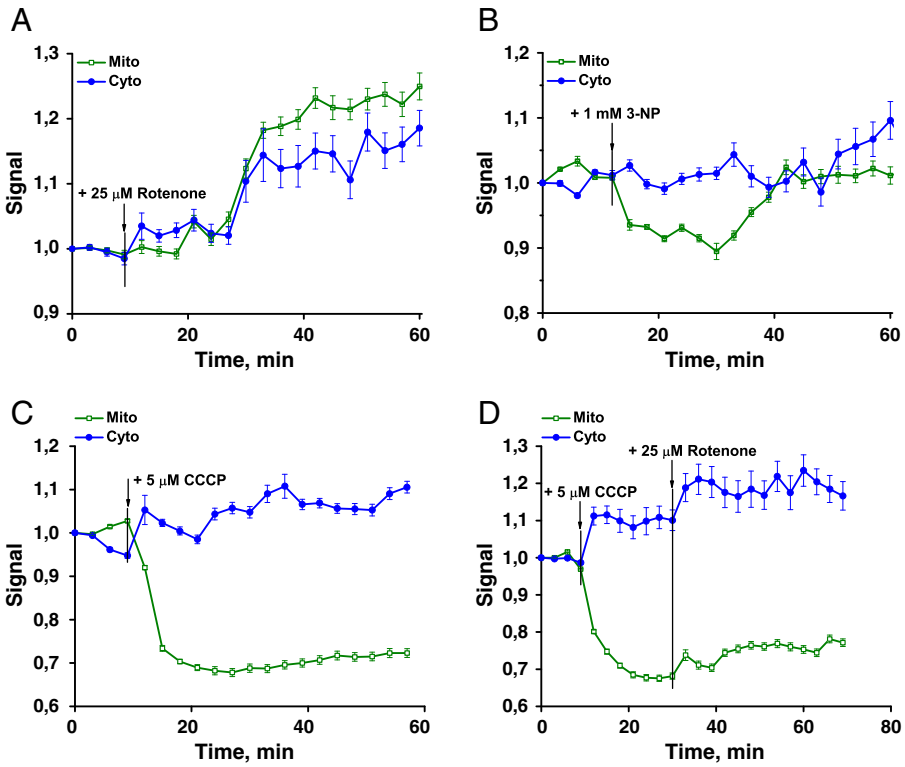

Fig. 4. RexYFP signal ($F490_{HyPer\text{-}C199S}/F490_{RexYFP}$ normalized to the initial value) in the cytoplasm (blue line) and in the mitochondria (green line) of HeLa cells after addition of A) 25 μM rotenone (signals were averaged from 36 cells with mito-localization of the sensor and 48 cells with cyto- in 3 experiments); B) 1 mM 3-NP (from 62 cells with mito- and 57 cells with cyto- in 4 experiments); C) 5 μM CCCP (from 38 cells with mito- and 49 cells with cyto- in 3 experiments); D) 5 μM CCCP with subsequent addition of 25 μM rotenone (from 42 cells with mito- and 37 cells with cyto- in 3 experiments). Error bars indicate standard error of mean.

NAD^+/NADH in the cytoplasm, [1] suggesting that under certain conditions NADPH could contribute to the changes in RexYFP signal.

RexYFP is sensitive to minimal changes in NADH. Why is it considered to be a NAD^+/NADH ratio sensor but not an NADH sensor? Since the NAD(H) pool exists mostly in an oxidized state, at least in the cytoplasm [3,32], NAD^+ concentration is some orders of magnitude higher compared to NADH. Therefore, although NAD^+ does not cause fluorescence changes in RexYFP, it can compete with NADH for the Rossmann-fold binding. Note that Peredox, even with its higher affinity for NADH, had been considered to sense NAD^+/NADH ratio rather than NADH.

cpYFP-based indicators are pH-sensitive. In fact, SypHer (HyPer-C199S), a pH probe with cpYFP chromophore, is a very good ratiometric green-emitting pH probe. RexYFP is no exception: it has perfect pH sensitivity, which could make NAD(H) state imaging problematic. Indeed, we found that many conditions we used in our experiments change pH in either cytoplasm, or mitochondria, or both. Surprisingly, pKa of HyPer and RexYFP differ, although they share the same cpYFP as a fluorophore. Therefore, the pH dependence profile depends not only on the particular cpFP used, but also on the domain fused to it. Most probably, the protein domain fused to cpYFP modifies the network of H-bonds used for proton transfer to and from Tyr of the chromophore. Nevertheless, the degree of fluorescence changes per pH unit in a range between 6.5 and 8.5 is very similar between RexYFP and HyPer. We therefore used SypHer signal to normalize RexYFP ratio changes.

To validate the utility of pH-normalized RexYFP signal for measuring intracellular NAD^+/NADH fluctuations, we compared the profiles/changes of RexYFP signal to those of Peredox head-to-head. Data obtained from two cell lines, HeLa and HEK293, expressing either Peredox or RexYFP, demonstrated comparable responses to the addition of pyruvate and lactate, inhibition of the respiratory chain by rotenone. While in general the amplitude and timing of the signals were similar for both of the sensors, we detected some differences. Specifically, Peredox showed more rapid response to NADH accumulation in the cytoplasm when cells were incubated with rotenone. A possible explanation lies in the higher affinity of Peredox for NADH. Other stimuli, such as pyruvate and lactate, elicited very similar responses in both probes in terms of timing and degree of change.

The very high affinity of Peredox for NADH precludes its use in the mitochondria. The affinity of RexYFP for NADH is lower by more than an order of magnitude. Our tests showed that RexYFP can be used as a mitochondrial NAD(H) redox state dynamics reporter. Normalizing mitoRexYFP signal to mitoSypHer signal, we determined effects of the respiratory chain uncoupling and ETC component inhibition.

CCCP, as a typical uncoupling agent, increases the proton permeability of membranes, which leads to uncoupling of the electron transport via ETC and ATP production [33,34]. As a result, electron transport rate reaches its maximum, leading to the fast oxidation of the mitochondrial NADH pool. We detected NADH increase in the cytoplasm (Fig. 4C, D). The effect of CCCP on the NADH pool was reduced by inhibiting complex I with rotenone. Unexpectedly, rotenone-induced RexYFP signal changes were faster in the cytoplasm than in the mitochondrial matrix.

We found that inhibition of complex II by 3-NP led to decreased NADH in the mitochondria, but not in the cytoplasm. Complex II delivers additional electrons into the quinone pool from succinate [35]. An explanation could be that complex I partially compensates for the lack of reducing equivalents from complex II in the respiratory chain. This leads to a greater consumption of NADH.

The results of mitoRexYFP experiments are in agreement with data obtained earlier using NADH sensor Frex. Frex demonstrated 3-NP-induced decrease of mitochondrial NADH levels and CCCP-induced NADH oxidation (but both in the cytoplasm and in the mitochondria) reversed by the inhibition of complex I [19]. However, Frex exists in three versions that differ in their affinity for NADH and direction of fluorescence changes. Two versions, Frex and C3L194K, were preferable to use in mitochondria and the other, FrexH, in the cytoplasm. Therefore, direct comparison between the two compartments using the same

probe was not possible. RexYFP can be used in both the cytoplasm and the mitochondrial matrix, better enabling comparison of the NAD(H) redox state in different compartments.

Summarizing, we developed the genetically encoded fluorescent sensor called RexYFP for detection of the NAD^+/NADH redox state. RexYFP is a reasonable alternative to existing sensors and is suitable for detecting the NAD(H) redox state in different cellular compartments. RexYFP is the only sensor that allows comparison of NAD^+/NADH ratio dynamics in both the mitochondria and the cytoplasm. Our results show that normalizing the signal of the sensor to the pH changes is a good strategy for overcoming pH-induced artifacts in imaging. However, a prospective direction would be substituting the cpYFP for a bright fluorescent protein that is insensitive or, at least, much less sensitive to pH changes.

Acknowledgements

This work was supported by the Russian Foundation for Basic Research (13-04-40333-H), a joint EMBL-RFBR grant (12-04-92427), Measures to Attract Leading Scientists to Russian Educational Institutions program (11.G34.31.0071), National Institute of Aging (grant R01AG040209) and the Molecular and Cell Biology program of Russian Academy of Sciences.

References

[1] R.L. Veech, L.V. Eggleston, H.A. Krebs, The redox state of free nicotinamide-adenine dinucleotide phosphate in the cytoplasm of rat liver, Biochem. J. 115 (1969) 609–619.
[2] M. Stubbs, R.L. Veech, H.A. Krebs, Control of the redox state of the nicotinamide-adenine dinucleotide couple in rat liver cytoplasm, Biochem. J. 126 (1972) 59–65.
[3] W. Ying, NAD^+ and NADH in cellular functions and cell death, Front. Biosci. 11 (2006) 3129–3148.
[4] C.C. Alano, W. Ying, R.A. Swanson, Poly(ADP-ribose) polymerase-1-mediated cell death in astrocytes requires NAD^+ depletion and mitochondrial permeability transition, J. Biol. Chem. 279 (2004) 18895–18902.
[5] C.C. Alano, P. Garnier, W. Ying, Y. Higashi, T.M. Kauppinen, R.A. Swanson, NAD^+ depletion is necessary and sufficient for poly(ADP-ribose) polymerase-1-mediated neuronal death, J. Neurosci. 30 (2010) 2967–2978.
[6] M. Ziegler, New functions of a long-known molecule. Emerging roles of NAD in cellular signaling, Eur. J. Biochem. 267 (2000) 1550–1564.
[7] F. Berger, M.H. Ramírez-Hernández, M. Ziegler, The new life of a centenarian: signalling functions of NAD(P), Trends Biochem. Sci. 29 (2004) 111–118.
[8] J. Rutter, M. Reick, L.C. Wu, S.L. McKnight, Regulation of clock and NPAS2 DNA binding by the redox state of NAD cofactors, Science 293 (2001) 510–514.
[9] H. Schneckenburger, M. Wagner, P. Weber, W.S. Strauss, R. Sailer, Autofluorescence lifetime imaging of cultivated cells using a UV picosecond laser diode, J. Fluoresc. 14 (2004) 649–654.
[10] S. Huang, A.A. Heikal, W.W. Webb, Two-photon fluorescence spectroscopy and microscopy of NAD(P)H and flavoprotein, Biophys. J. 82 (2002) 2811–2825.
[11] G.H. Patterson, S.M. Knobel, P. Arkhammar, O. Thastrup, D.W. Piston, Separation of the glucose-stimulated cytoplasmic and mitochondrial NAD(P)H responses in pancreatic islet beta cells, Proc. Natl. Acad. Sci. U. S. A. 97 (2000) 5203–5207.
[12] K.A. Kasischke, H.D. Vishwasrao, P.J. Fisher, W.R. Zipfel, W.W. Webb, Neural activity triggers neuronal oxidative metabolism followed by astrocytic glycolysis, Science 305 (2004) 99–103.
[13] Q. Yu, A.A. Heikal, Two-photon autofluorescence dynamics imaging reveals sensitivity of intracellular NADH concentration and conformation to cell physiology at the single-cell level, J. Photochem. Photobiol. B 95 (2009) 46–57.
[14] S. Lisby, R. Gniadecki, H.C. Wulf, UV-induced DNA damage in human keratinocytes: quantitation and correlation with long-term survival, Exp. Dermatol. 14 (2005) 349–355.
[15] R. Gniadecki, T. Thorn, J. Vicanova, A. Petersen, H.C. Wulf, Role of mitochondria in ultraviolet-induced oxidative stress, J. Cell. Biochem. 80 (2000) 216–222.
[16] A. Hopt, E. Neher, Highly nonlinear photodamage in two-photon fluorescence microscopy, Biophys. J. 80 (2001) 2029–2036.
[17] G.H. Patterson, D.W. Piston, Photobleaching in two-photon excitation microscopy, Biophys. J. 78 (2000) 2159–2162.
[18] Y.P. Hung, J.G. Albeck, M. Tantama, G. Yellen, Imaging cytosolic NADH-NAD^+ redox state with a genetically encoded fluorescent biosensor, Cell Metab. 14 (2011) 545–554.
[19] Y. Zhao, J. Jin, Q. Hu, H.M. Zhou, J. Yi, Z. Yu, L. Xu, X. Wang, Y. Yang, J. Loscalzo, Genetically encoded fluorescent sensors for intracellular NADH detection, Cell Metab. 14 (2011) 555–566.
[20] K.J. McLaughlin, C.M. Strain-Damerell, K. Xie, D. Brekasis, A.S. Soares, M.S. Paget, C.L. Kielkopf, Structural basis for NADH/NAD^+ redox sensing by a Rex family repressor, Mol. Cell 38 (2010) 563–575.
[21] E. Wang, M.C. Bauer, A. Rogstam, S. Linse, D.T. Logan, C. von Wachenfeldt, Structure and functional properties of the *Bacillus subtilis* transcriptional repressor Rex, Mol. Microbiol. 69 (2008) 466–478.
[22] V.V. Belousov, A.F. Fradkov, K.A. Lukyanov, D.B. Staroverov, K.S. Shakhbazov, A.V. Terskikh, S. Lukyanov, Genetically encoded fluorescent indicator for intracellular hydrogen peroxide, Nat. Methods 3 (2006) 281–286.
[23] J. Berg, Y.P. Hung, G. Yellen, A genetically encoded fluorescent reporter of ATP:ADP ratio, Nat. Methods 6 (2009) 161–166.
[24] B. Simen Zhao, Y. Liang, Y. Song, C. Zheng, Z. Hao, P.R. Chen, A highly selective fluorescent probe for visualization of organic hydroperoxides in living cells, J. Am. Chem. Soc. 132 (2010) 17065–17067.
[25] J. Wang, J. Karpus, B.S. Zhao, Z. Luo, P.R. Chen, C. He, A selective fluorescent probe for carbon monoxide imaging in living cells, Angew. Chem. Int. Ed. Engl. 51 (2012) 9652–9656.
[26] D. Poburko, J. Santo-Domingo, N. Demaurex, Dynamic regulation of the mitochondrial proton gradient during cytosolic calcium elevations, J. Biol. Chem. 286 (2011) 11672–11684.
[27] E.A. Sickmier, D. Brekasis, S. Paranawithana, J.B. Bonanno, M.S. Paget, S.K. Burley, C.L. Kielkopfl, X-Ray structure of a Rex-family repressor/NADH complex insights into the mechanism of redox sensing, Structure 13 (2005) 43–54.
[28] M.W. Slein, Methods of Enzymatic Analysis, Academic Press, New York, 1963.
[29] H. Jörnvall, B. Persson, M. Krook, S. Atrian, R. Gonzàlez-Duarte, J. Jeffery, D. Ghosh, Short-chain dehydrogenases/reductases (SDR), Biochemistry 34 (1995) 6003–6013.
[30] R.C. Poole, A.P. Halestrap, Transport of lactate and other monocarboxylates across mammalian plasma membranes, Am. J. Physiol. 264 (1993) 761–782.
[31] A.V. Zima, J. Kockskämper, R. Mejia-Alvarez, L.A. Blatter, Pyruvate modulates cardiac sarcoplasmic reticulum Ca^{2+} release in rats via mitochondria-dependent and -independent mechanisms, J. Physiol. 550 (2003) 765–783.
[32] D.H. Williamson, P. Lund, H.A. Krebs, The redox state of free nicotinamide-adenine dinucleotide in the cytoplasm and mitochondria of rat liver, Biochem. J. 103 (1967) 514–527.
[33] O.H. LeBlanc, The effect of uncouplers of oxidative phosphorylation on lipid bilayer membranes: carbonylcyanide m-chlorophenylhydrazone, J. Membr. Biol. 4 (1971) 227–251.
[34] P.H. Lou, B.S. Hansen, P.H. Olsen, S. Tullin, M.P. Murphy, M.D. Brand, Mitochondrial uncouplers with an extraordinary dynamic range, Biochem. J. 407 (2007) 129–140.
[35] K.S. Oyedotun, B.D. Lemire, The quaternary structure of the *Saccharomyces cerevisiae* succinate dehydrogenase. Homology modeling, cofactor docking, and molecular dynamics simulation studies, J. Biol. Chem. 279 (2004) 9424–9431.